Received: 14 December 2021 | Revised: 7 February 2022 | Accepted: 9 February 2022

DOI: 10.1111/cas.15300

Cancer Science WILEY

ORIGINAL ARTICLE

DCAF13 promotes breast cancer cell proliferation by ubiquitin inhibiting *PERP* expression

Bao-Qian Shan[1] | Xiao-Min Wang[2] | Li Zheng[3] | Yao Han[2] | Jie Gao[2] | Meng-Dan Lv[2] | Yi Zhang[2] | Yi-Xuan Liu[2] | Han Zhang[2] | Hao-Sa Chen[2] | Lei Ao[2] | Yin-Li Zhang[4] | Xiang Lu[5] | Zhong-Jie Wu[5] | Ying Xu[2] | Xuan Che[6] | Michal Heger[7,8] | Shu-Qun Cheng[9,10] | Wei-Wei Pan[2,10] | Xin Zhang[1]

[1]College of Forest and Biotechnology, Zhejiang A & F University, Hangzhou, China

[2]Department of Cell Biology, College of Medicine, Jiaxing University, Jiaxing, China

[3]The Key Laboratory, The Second Affiliated Hospital of Jiaxing University, Jiaxing, China

[4]Department of Obstetrics and Gynecology, Sir Run Run Shaw Hospital, School of Medicine, Zhejiang University, Hangzhou, China

[5]Department of Cardiothoracic Surgery, Affiliated Hospital of Jiaxing University, Jiaxing, China

[6]Department of Anesthesiology, Jiaxing Maternity and Child Health Care Hospital, Affiliated with Women and Children Hospital, Jiaxing University, Jiaxing, China

[7]Department of Pharmaceutics, Jiaxing Key Laboratory for Photonanomedicine and Experimental Therapeutics, College of Medicine, Jiaxing University, Jiaxing, China

[8]Department of Pharmaceutics, Utrecht Institute for Pharmaceutical Sciences, Utrecht University, Utrecht, The Netherlands

[9]Department of Hepatic Surgery VI, Eastern Hepatobiliary Surgery Hospital, Second Military Medical University, Shanghai, China

[10]G60 STI Valley Industry & Innovation Institute, Jiaxing University, Jiaxing, China

Correspondence
Wei-Wei Pan, College of Medicine, Jiaxing University, 314001 Jiaxing, China.
Email: wwpan@mail.zjxu.edu.cn

Xin Zhang, College of Forest and Biotechnology, Zhejiang A & F University, 311300 Hangzhou, China.
Email: zhangxins@126.com

Funding information
The National Natural Science Foundation of China (Grant Number: 31871402, 31701260), the Natural Science Foundation of Zhejiang Province (Grant Number: LY21H160047, LY17H160060,

Abstract

Evolutionarily conserved DDB1-and CUL4-associated factor 13 (DCAF13) is a recently discovered substrate receptor for the cullin RING-finger ubiquitin ligase 4 (CRL4) E3 ubiquitin ligase that regulates cell cycle progression. DCAF13 is overexpressed in many cancers, although its role in breast cancer is currently elusive. In this study we demonstrate that DCAF13 is overexpressed in human breast cancer and that its overexpression closely correlates with poor prognosis, suggesting that DCAF13 may serve as a diagnostic marker and therapeutic target. We knocked down *DCAF13* in breast cancer cell lines using CRISPR/Cas9 and found that *DCAF13* deletion markedly

Abbreviations: APC, APC regulator of WNT signaling pathway; ATP13A4, ATPase 13A4; CCK8, cell counting kit-8; CD44, CD44 molecule (Indian blood group); CDK, cyclin-dependent kinase; CDT1, chromatin licensing and DNA replication factor 1; CI, confidence interval; COL5A3, collagen type V alpha 3 chain; CRL4, cullin RING-finger ubiquitin ligase 4; DCAF13, DDB1-and CUL4-associated factor 13; DDB1, DCAF13 and DNA damage-binding protein 1; Dicer 1, dicer 1, ribonuclease III; DVL1, dishevelled segment polarity protein 1; GOLPH2, Golgi reassembly stacking protein 2; GSK-3β, glycogen synthase kinase 3 beta; HP1, Chromobox 5; HR, hazard ratio; IF, immunofluorescence; IHC, immunohistochemistry; MMP13, matrix metallopeptidase 13; MYL9, myosin light chain 9; NF2, moesin-ezrin-radixin like (MERLIN) tumor suppressor; NOXA, phorbol-12-myristate-13-acetate-induced protein 1; OS, overall survival; p-CHK1, phosphorylated-checkpoint kinase 1; PERP, P53 apoptosis effector related to PMP22; p-H2AX, phosphorylated-H2A.X variant histone; PMP22, peripheral myelin protein 22; PTEN, phosphatase and tensin homolog; RASGRP2, RAS guanyl releasing protein 2; RASSF4, Ras association domain family member 4; RBP, RNA-binding protein; RNAseq, RNA sequencing; SLC22A18, solute carrier family 22 member 18; TCGA, The Cancer Genome Atlas; TNBC, triple-negative breast cancer; β-catenin, cadherin associated protein, beta 1.

Bao-Qian Shan, Xiao-Min Wang, and Li Zheng contributed equally to this work.

LGD21H160003, LZ20H16004), the Jiaxing Science and Technology Bureau project (Grant Number: 2020AD10018, 2020AD30073, 00320117AL), the Jiaxing Key Laboratory for Photonanomedicine and Experimental Therapeutics (Grant Number: 12.2019), the Zhejiang Provincial Foreign Expert Grant (Grant Number: 12.2018), the Dutch Cancer Foundation (Grant Number: KWF, 10666), the Jiaxing University Scientific Research Start-up project (Grant Number: CD70519018), the National College Student Innovation and Entrepreneurship Training Program (Grant Number: 202010354043, 202010354042, 2020R417015, 202110354015, 2021R417023, 2021R417028, 202113291002, 202113291003)

reduced breast cancer cell proliferation, clone formation, and migration both *in vitro* and *in vivo*. In addition, *DCAF13* deletion promoted breast cancer cell apoptosis and senescence, and induced cell cycle arrest in the G1/S phase. Genome-wide RNAseq analysis and western blotting revealed that loss of *DCAF13* resulted in both mRNA and protein accumulation of p53 apoptosis effector related to PMP22 (PERP). Knockdown of *PERP* partially reversed the hampered cell proliferation induced by DCAF13 knockdown. Co-immunoprecipitation assays revealed that DCAF13 and DNA damage-binding protein 1 (DDB1) directly interact with PERP. Overexpression of DDB1 significantly increased PERP polyubiquitination, suggesting that $CRL4^{DCAF13}$ E3 ligase targets PERP for ubiquitination and proteasomal degradation. In conclusion, DCAF13 and the downstream effector PERP occupy key roles in breast cancer proliferation and potentially serve as prognostics and therapeutic targets.

KEYWORDS
breast cancer, CRL4, DCAF13, DDB1, PERP, post-translational modification, ubiquitin E3 ligase

1 | INTRODUCTION

Breast cancer is one of the leading causes of cancer-related deaths among females worldwide.[1] In 2020, breast cancer surpassed lung cancer as the leading cause of global cancer incidence.[2] Although early stage breast cancer has a good prognosis following surgery and chemotherapy, approximately 90% of deaths among patients with breast cancer are due to recurrence and distant metastasis of the primary tumor.[3] The mechanisms underlying breast cancer development and recurrence should therefore be investigated to develop effective diagnostic and therapeutic modalities.

The cullin RING-finger ubiquitin ligase 4 (CRL4) is an important component of the ubiquitin–proteasome system that contributes to tumorigenesis through multiple mechanisms, including involvement in DNA damage and repair, cell cycle regulation, and the ubiquitination of oncoproteins and tumor suppressors.[4,5] CUL4 uses DNA damage-binding protein 1 (DDB1) as a linker to interact with DDB1- and CUL4-associated factors (DCAFs), which serve as substrate receptors of the CRL4 E3 ligase.[6,7] Through different DCAFs, CRL4 E3 ligases recognize a number of substrates for ubiquitination and degradation, such as the tumor repressor LAST1/2,[8] CDT1,[9,10] dicer 1,[11] and NF2,[12] and contribute to the occurrence and development of tumors.

DDB1- and CUL4-associated factor 13 has recently been identified as a substrate recognition receptor for CRL4 E3 ligases that mediates pre-implantation embryonic development and mammalian oocyte growth.[13,14] *DCAF13* has also attracted growing interest in cancer research. In osteosarcoma cells, the CRL4B–DCAF13 E3 ligase complex specifically targets the tumor suppressor phosphatase and tensin homolog (*PTEN*) for degradation.[15] Moreover, DCAF13 is frequently amplified in hepatocellular carcinoma patients, and increased expression of *DCAF13* reportedly defined a subgroup of hepatocellular carcinoma patients with significantly poor prognosis.[16,17] DCAF13 also acts as a novel RNA-binding protein (RBP) that contributes to triple-negative breast cancer (TNBC) metastasis.[18] Accordingly, DCAF13 is central in cancer biology and potentially serves as a biomarker for more robust staging of cancer patients. In breast cancer, however, the exact role of DCAF13 is currently unclear.

In this study, we found that *DCAF13* was overexpressed in malignant human breast tissue and breast cancer cell lines. Deletion of *DCAF13* inhibited breast cancer cell growth, colony formation, and migration and inhibited the growth of human breast cancer xenografts in mice. We further observed that CRL4B-DCAF13 E3 ligase facilitates polyubiquitination of PERP, which acts as the transcriptional downstream protein of p53 and p63. Accordingly, several important functions of DCAF13 were unveiled in the context of breast cancer and PERP was identified as a novel substrate of $CRL4^{DCAF13}$ E3 ligase.

2 | MATERIALS AND METHODS

2.1 | Cell culture and stable cell line generation

Mouse breast cancer cell lines 4T07, 4T1, 168FARN, and 67NR; mouse melanoma cell line B16; human breast cancer cell lines MCF-7 and MDA-MB-231; mouse colon cancer cell line MC38; human colon cancer cell line HCT116; thyroid squamous cancer cell line SCC7; mouse glioma cell line GL261; mouse pancreatic cancer cell line Panco2; mouse lung cancer cell line LLC1; human lung cancer cell line H1299; mouse bladder cancer cell line MB49; human ovarian cancer cell lines A2780 and C13; and human normal ovarian epithelial cell line IOSE were purchased from American Type Culture Collection. The cell lines were cultured in DMEM (Gibco Life Technologies) supplemented with 10% FBS (Gibco Life Technologies) and 1% penicillin–streptomycin (Gibco Life Technologies) at 37 °C in an atmosphere composed of 95% air and 5% CO_2 (standard culture conditions).

DDB1- and CUL4-associated factor 13- or PERP-deficient cells were established using CRISPR/Cas9 technology (Sup-1). DCAF13 and PERP guide RNA sequences is in Table S1.

2.2 | Cell proliferation, colony formation, and invasion assay

For cell growth curve analysis, cells were seeded in six-well plates at a density of 100,000 cells/well. At 24 h, 48 h, and 72 h the total number of cells in each well was counted in triplicate. Cell viability was determined using the Cell Counting Kit-8 (MCE) according to the manufacturer's instructions.

For colony formation experiments, each six-well plate was coated with 1.5 ml of bottom agar (0.5% Difco agar Noble in standard culture medium). Approximately 2500–5000 cells were suspended in 1.5 ml of top agar (0.35% Difco agar Noble in standard culture medium) and transferred into a well. The plates were incubated for 21 days at standard culture conditions before staining with 0.5% crystal violet (Sangon Biotech) for quantification.

The invasion assays were performed by placing 5000 cells/well into the upper chamber of the Transwell unit (Corning) in serum-free medium. Fully supplemented growth medium containing 10% FBS was placed in the lower chamber. After 24 h, cells in the upper chamber were completely removed with a cotton swab, and the migrated cells attached to the bottom side were fixed in 100% methanol and stained with hematoxylin and eosin (SignaGen). The stained cells were counted using ImageJ software (National Institutes of Health).

2.3 | Antibodies, western blotting, and co-immunoprecipitation

Whole cell lysates were prepared with RIPA lysis buffer (Beyotime), denatured at 95 °C for 10 min, separated using SDS-PAGE, and transferred to PVDF membranes (Millipore). The target proteins were detected by primary antibodies and horseradish peroxidase-linked secondary antibodies (Proteintech) (Table S2). The bands were revealed using an enhanced chemiluminescence detection kit (Millipore).

For co-immunoprecipitation experiments, the plasmid was transfected into 293A cells that were subsequently lysed in RIPA lysis buffer and centrifuged. The supernatants were immunoprecipitated with the respective antibodies for 3 h at 4 °C, followed by incubation with Protein A/G agarose beads (Thermo Fisher Scientific) for 1 h at 4 °C. The immunocomplexes were then washed six times with RIPA buffer containing 5% Tween 80 and assayed by Western blotting.

2.4 | Breast tumor biopsies

Paraffin-embedded human breast cancer tissue microarrays (TMAs; $N = 75$ patients) were purchased from Fanpu Biotech, Inc. Each specimen in these TMAs was represented in two cores on the slide, each measuring 1.5 mm in diameter. Tumor type, staging, and classification data are presented in Tables S3 and S7.

Furthermore, fresh breast tumor tissue and adjacent non-neoplastic tissue ($N = 10$) were biopsied from patients who had been admitted to the Jiaxing University First Affiliated Hospital (Jiaxing, Zhejiang, China). All patients or their legal representatives signed an informed consent document. Tumor type, staging, and classification data are presented in Table S8. Approval was obtained from the institutional review board of the Jiaxing University First Affiliated Hospital Ethics Committee (Registration No. LS2021-KY-047).

2.5 | Immunohistochemistry and immunofluorescence

Immunohistochemistry (IHC) and immunofluorescence (IF) were performed as described previously.[19] Briefly, IHC was performed on the paraffin-embedded tissue microarray using anti-DCAF13, anti-p-histone H3, and anti-cleaved caspase3 antibodies (Table S2). Protein expression levels were ascertained by multiplying the percentage of positive cells by immunostaining intensity. The percentages were allocated scores as follows: nonpositive cells as 0 points, and 1%–25% as 1, 26%–50% as 2, 51%–75% as 3, and 76%–100% as 4 points. The staining intensity was graded as follows: no positive staining as 0 points, while weak staining as 1, moderate staining as 2, and strong staining as 3 points. The final scores were calculated and classified as weak (0–3), moderate (4–8), and high levels (9–12) of expression.

For immunofluorescence analysis, cultured cells were washed with PBS, fixed with 4% formaldehyde, blocked with 1% BSA, and incubated with primary antibodies against p-histone H3, pH2AX, p-CHK1, β-catenin, GOLPH2, nucleophosmin, and HP1 (Table S2). After washing, the cells were incubated with Alexa488-conjugated secondary antibodies (Solarbio) and counterstained with DAPI (Beyotime). Digital images were acquired using a laser scanning confocal microscope (Olympus).

2.6 | Quantitative real time PCR

Total RNA was extracted from cultured cells using TRIzol Reagent (Invitrogen Life Technologies). The extracted RNA was reverse-transcribed into cDNA using PrimeScript RT Reagent Kit (Takara). Real-time PCR analysis was performed using SYBR Green Master Mix kit (Takara) and an Applied 7300 Real-time PCR system (Eppendorf). Relative mRNA levels of each gene were normalized to household gene levels (β-actin). Experiments were performed in triplicate. The primers are detailed in Table S4.

2.7 | RNA interference

The siRNA oligonucleotides corresponding to the target sequence of PERP and SLC22A18 were designed and synthesized by

GenePharma (Table S5). A negative control siRNA (GenePharma) was included in the experiments. Breast cancer cells were seeded into six-well plates at a density of 500,000 cells/well. The siRNA sequences were transfected into cells using the GP-siRNA-Mate Plus reagent (GenePharma) according to the manufacturer's instructions.

2.8 | Mice and xenograft models

All mouse experiments were conducted in accordance with national animal welfare regulations following ethics approval by Laboratory Animal Ethics Committee of JXMC (Registration No. JUMC2021-085). One million cells were subcutaneously injected in both flanks of 8-week-old nude female mice (Animal Center of the Chinese Academy of Sciences, Shanghai, China). Tumor volumes were measured every 2 days and calculated according to the following formula: volume (mm^3) = ½ × length × $width^2$. After 26 days, the mice were sacrificed and sub-skin grafts were collected for Western blot and immunohistochemistry analyses.

2.9 | Flow cytometric analyses of apoptosis and cell cycle

For the apoptosis assay, cells were incubated with Annexin V-PE and propidium iodide (BD Biosciences) and analyzed using FC500 flow cytometer (Beckman Coulter). Cell cycle analysis was performed following propidium iodide staining using a CycleTest Plus DNA Reagent Kit (BD Biosciences) according to the manufacturer's instructions. The results were evaluated with a FACScan flow cytometer (BD Biosciences). The number of cells in each phase were determined.

2.10 | Senescence-associated β-galactosidase activity assay

Cell senescence analysis was performed using a senescence β-galactosidase staining kit (Cell Signaling Technology). A total of 100,000 cells were stained with freshly prepared senescence-associated β-galactosidase overnight at 37 °C and counterstained with eosin. The number of blue-stained senescent cells in randomly selected fields was expressed as a percentage of the total cells.

2.11 | Statistical analysis

All *in vitro* assays were performed at least three times. Statistical analysis was performed using GraphPad Prism software (GraphPad Software). Groups were compared using a nonparametric test unless otherwise noted. The log-rank test was applied to Kaplan–Meier analysis in Figure 1D. Data were considered significant at $p < 0.05$. Levels of significance are represented with asterisks as follows: $^{*}p < 0.05$, $^{**}p < 0.01$, and $^{***}p < 0.001$.

3 | RESULTS

3.1 | DCAF13 is overexpressed in human breast cancer tissue and cells

To investigate DCAF13 expression patterns in breast cancer tissue, immunohistochemical analysis was performed on the breast cancer tissue microarrays. Based on staining intensity, we classified the samples into five groups with increasing staining intensity from the weakest (−) to the strongest (++++) (Figure 1A). Positive DCAF13 staining was observed in 48 of 72 (66.7%) malignant breast cancer samples, which exhibited + (30.7%), ++ (21.3%), +++ (6.7%), and ++++ (5.3%) staining intensity. Partial or no DCAF13 staining was observed in normal breast cancer tissue. The tissue microarray analysis was followed up with Western blot analysis in 10 pairs of fresh breast tumor tissue and adjacent non-neoplastic tissue obtained from patients at the Jiaxing University First Affiliated Hospital. DCAF13 was overexpressed in seven of 10 breast cancer biopsies compared to nonmalignant tissue (Figure 1B). These results confirm that DCAF13 is overexpressed in the majority of breast cancer patients.

We further investigated *DCAF13* expression using the data in TCGA database. The clinical data of 1085 breast cancer patients from TCGA database are presented in Tables S6 and S7. We found that *DCAF13* expression was significantly elevated in breast cancer compared to healthy tissues ($p = 1.1 \times 10^{-41}$; Figure 1C). The OS in the *DCAF13* high-expression group was significantly worse than in the *DCAF13* low-expression group ($p = 0.016$; Figure 1D). Although no significant differences in DCAF13 expression were observed according to clinical stage ($p = 0.40$) (Figure S1A), *DCAF13* expression was independently associated with OS (HR 1.05, CI 1.12–1.90, $p = 0.004$; Figure S1B), suggesting that *DCAF13* expression is an independent predictor of OS in breast cancer patients.

Western blot and RT-PCR analyses of different cell lines verified that DCAF13 was overexpressed in the majority of breast cancer cell lines (4T07, 4T1, MCF-7, and MDA-MB-231), and particularly 4T1 and MCF-7 cells, compared to nonmalignant epithelial (IOSE) cells and tumor cells derived from other cancer types (Figure 1E,F). Accordingly, breast cancer cell lines are comparable to human breast cancer tissue in terms of DCAF13 overexpression.

3.2 | *DCAF13* deletion inhibits breast cancer cell proliferation, colony formation, and cell migration *in vitro*

We eliminated *DCAF13* in breast cancer cell lines (4T1, 4T07, and MCF-7) by CRISPR/Cas9. Although it was very challenging to obtain complete *DCAF13* knockout clones, two clones with a *DCAF13* deletion (KO19# and KO31#) had significantly lower DCAF13 protein expression levels (Figures 2A and S1D,E). Compared wild-type cells, *DCAF13* deletion led to a remarkable reduction in cell growth (Figure 2B–D). Correspondingly, the expression of cell proliferation marker p-histone H3 was also diminished in *DCAF13*-deficient cells

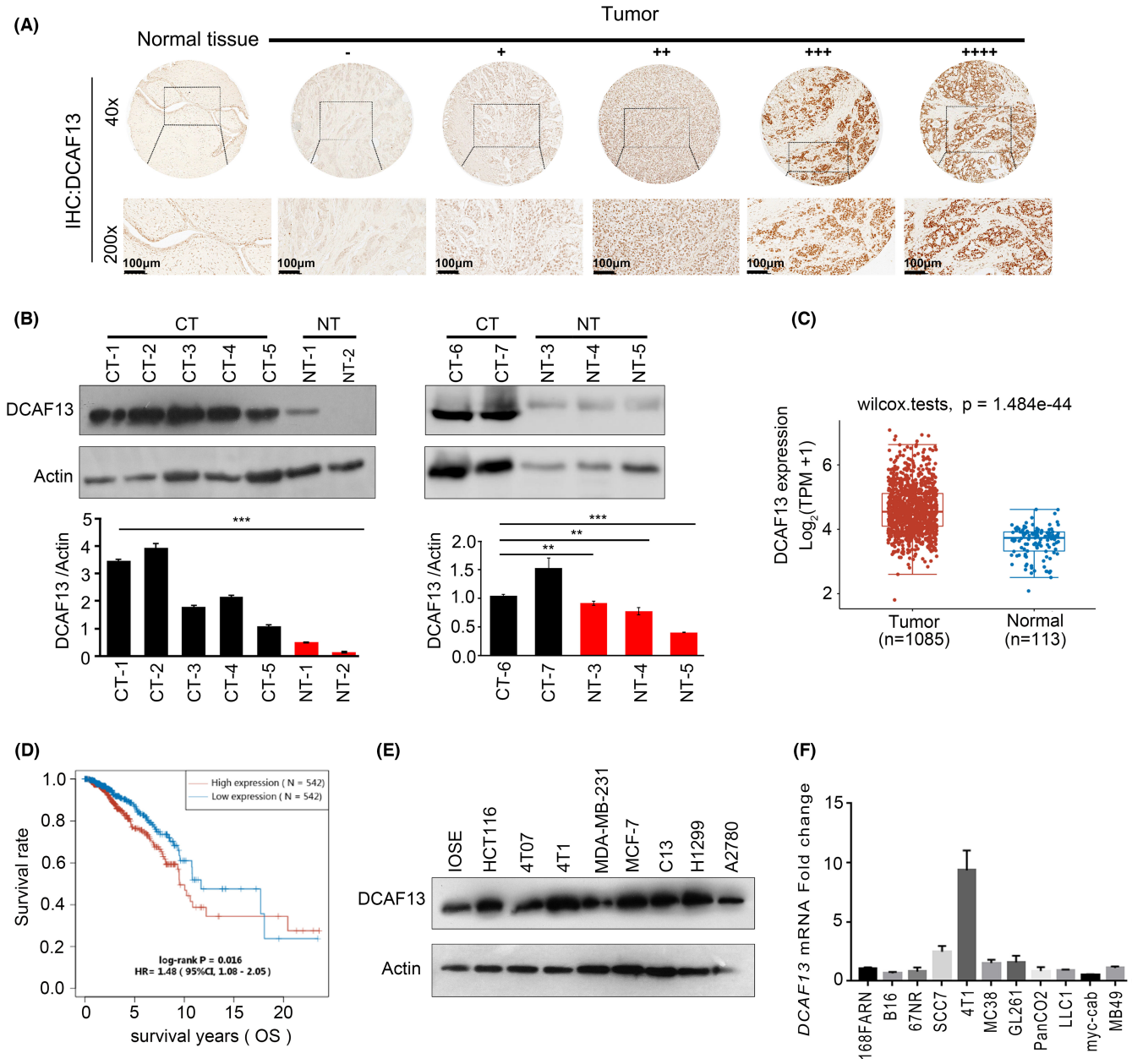

FIGURE 1 Aberrant expression of DCAF13 in breast cancer. (A) Expression of DCAF13 in human breast cancer tissue microarrays (40×, 200×). Representative images of DCAF13 immunohistochemistry staining of normal breast tissue ($N = 3$) and tumor tissue ($N = 72$). The staining intensity of DCAF13 in breast cancer was graded as negative (–) and positive, from the weakest to the strongest (+, ++, +++, ++++). (B) Western blot analysis of DCAF13 expression in breast tumor tissues and adjacent noncancerous tissues. CT, cancerous tissue; NT, noncancerous tissue. (C) *DCAF13* is typically overexpressed in breast cancer tissue as derived from the TCGA dataset (tumor tissue, $N = 1085$; normal tissue, $N = 113$). (D) High expression levels of DCAF13 were correlated with poorer overall survival in breast cancer patients compared to low expression levels ($N = 542$ per group, log-rank test, $p = 0.016$). (E) Ovarian cancer cells (A2780 and C13), colon cancer cells (HCT116), mouse breast cancer cells (4T07, 4T1), human breast cancer cells (MCF-7, MDA-MB-231), lung cancer cells (H1299), and immortalized human normal ovarian epithelial cells (IOSE) were subjected to immunoblot analysis using antibodies against DCAF13 and actin. (F) RT-PCR analysis of *DCAF13* expression in the indicated cancer cells. The fold change is relative to actin expression levels

(Figure 2A,I). Colony formation assays further showed that *DCAF13* deletion reduced the number of colonies formed (Figures 2E–G and S1D,E). Moreover, Transwell assays demonstrated that *DCAF13* deletion markedly suppressed the migration capacity of 4T07 and 4T1 cells (Figure 2H). These results demonstrate that DCAF13 is required for breast cancer cell proliferation and migration.

3.3 | *DCAF13* deletion promotes breast cancer cell cycle, apoptosis, and senescence

To further elucidate the mechanism underlying the inhibition of cell proliferation by *DCAF13* deletion, flow cytometry was employed to analyze the cell cycle in 4T1 and 4T07 cells. Compared to wild-type

breast cancer cells, *DCAF13* deletion significantly increased the number of cells in the G1 phase while decreasing the fraction in the S phase (Figure 3A). P16, p21, and p27 are cyclin-dependent kinase inhibitors that negatively regulate the cell cycle by blocking the activation of the CDK/cyclin complex. The expression levels of p21, p16, and p27 were significantly increased in *DCAF13* knockout cells (Figure 3B,C), suggesting that *DCAF13* suppression modulates the cell cycle via upregulation of p16, p21, and p27. Correspondingly,

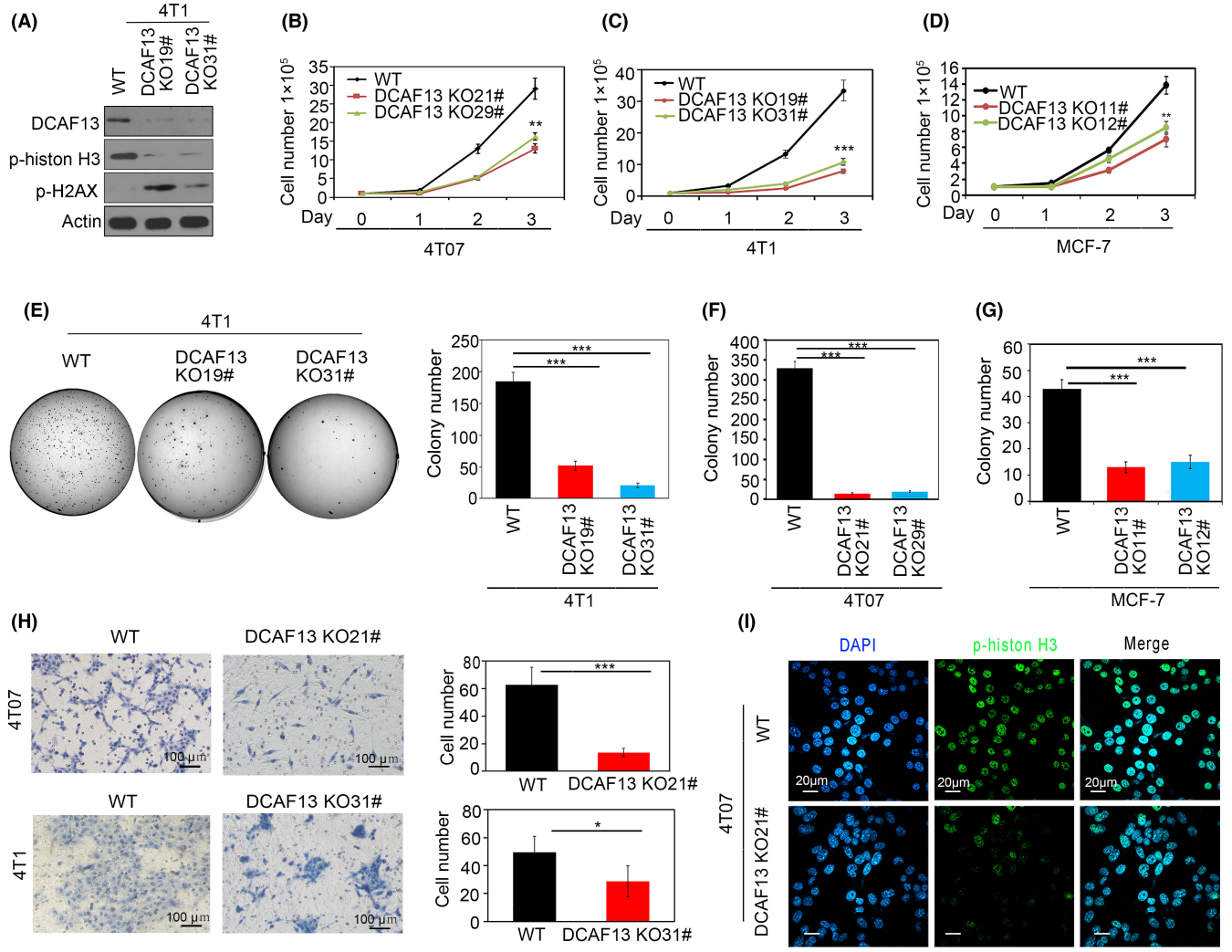

FIGURE 2 *DCAF13* deletion inhibits breast cancer cell growth and metastasis. (A) Deletion of *DCAF13* was confirmed at the protein level in different clones of 4T1 cells by immunoblotting. *DCAF13* deletion decreased the expression of p-histone H3 and increased the expression of p-H2AX. (B–D) *DCAF13* deletion inhibits 4T07 (B), 4T1(C), and MCF-7 (D) breast cancer cell growth. Cells (100,000) were plated in six-well culture dishes and cells were counted on days 1, 2, and 3. The data ($N = 3$ per cell line) are plotted as mean ± standard error (SE). $^{**}p < 0.01$, $^{***}p < 0.001$ (nonparametric test). (E–G) *DCAF13* deletion inhibits colony formation in 4T1 (E), 4T07 (F), and MCF-7 (G) cells. Data are presented as mean ± SE for $N = 3$ per cell line. $^{***}p < 0.001$. (H) *DCAF13* deletion inhibits 4T07 (upper panel) and 4T1 (lower panel) cell migration in a Transwell setup during 24-h culture. Cells were counterstained with hematoxylin and eosin. Positive cells were quantified using Image-J software. Data are presented as mean ± SE for $N = 3$ per cell line. $^{*}p < 0.05$, $^{***}p < 0.001$ (nonparametric test). (I) Immunofluorescence analysis of p-histone H3 (green) levels in 4T07 WT and DCAF13-deficient cells. Nuclei are counterstained with DAPI (blue)

FIGURE 3 Effects of *DCAF13* deletion on the cell cycle, cell senescence, and apoptosis in breast cancer cells. (A) Cell cycle distribution in different phases was analyzed by flow cytometry (left panels) in 4T07 and 4T1 cells. The percentage of cells in the G1, S, and G2 phase was analyzed using ModFitLT software (right panel). $^{**}p < 0.01$ (nonparametric test). (B) Western blot analysis of the expression of p21 in wild-type and *DCAF13* knockout breast cancer (4T07 and 4T1) cells. (C) RT-PCR analysis of the expression of *p27* and *p16* in wild-type and *DCAF13* knockout breast cancer cells. $^{**}p < 0.01$, $^{***}p < 0.001$ (nonparametric test). (D) Flow cytometric analysis of the mode of cell death in 4T07 and 4T1 cells. Representative flow cytograms are presented (left panel). The percentage of Annexin V-positive apoptotic cells was quantified (right panel). $^{**}p < 0.01$, $^{***}p < 0.001$ (nonparametric test). (E) Cell senescence as detected by SA-β-galactosidase staining in 4T07 cells shown qualitatively (left) and quantitatively (right). $^{**}p < 0.01$ (nonparametric test). Data are plotted as mean ± SD based on $N \geq 3$ experiments

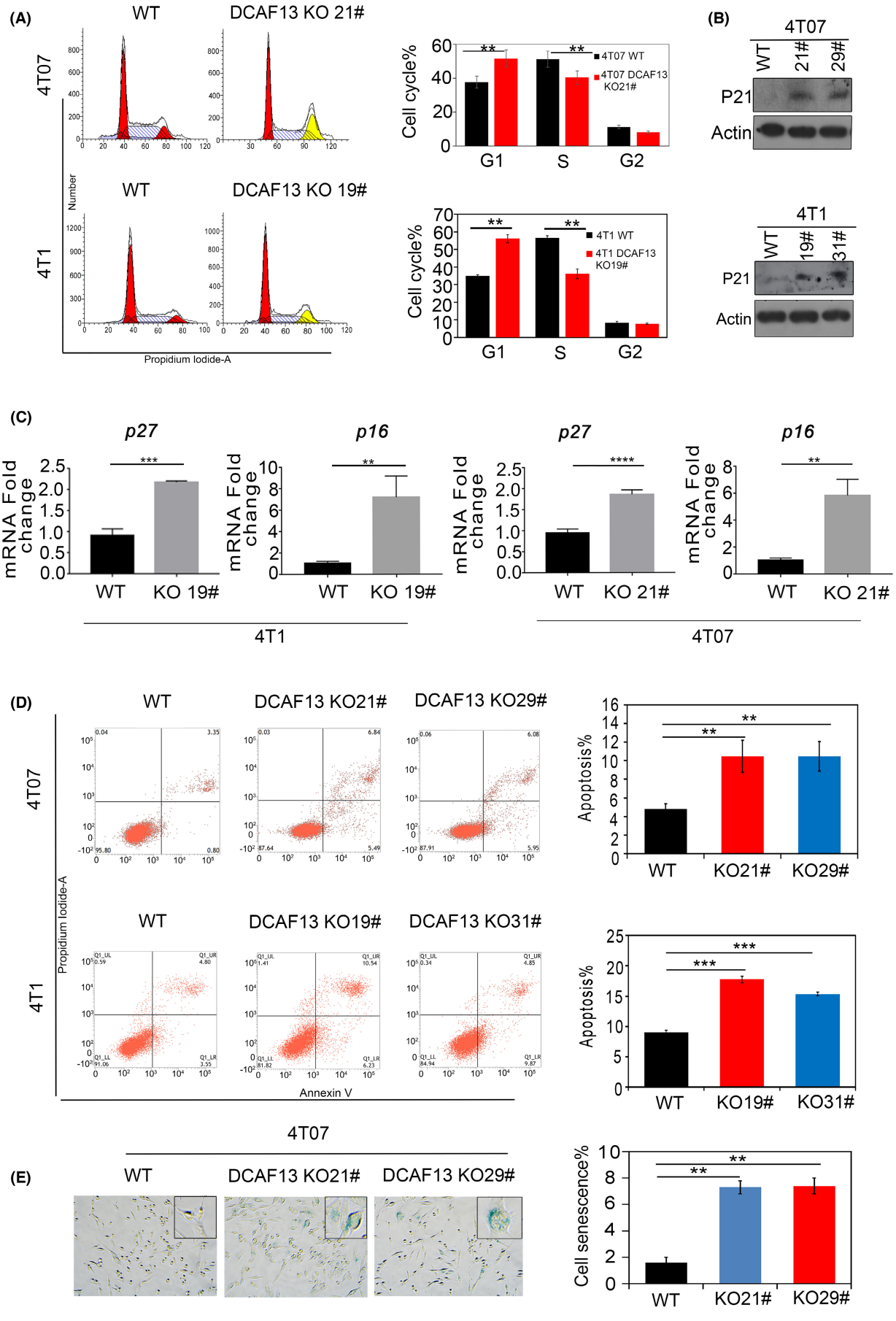

the rate of apoptosis in *DCAF13* knockout cells was increased (Figure 3D). Also, an increased number of *DCAF13* knockout cells exhibited elevated SA-β-galactosidase staining (Figure 3E). Taken together, these results suggest that the deletion of *DCAF13* inhibits breast cancer cell proliferation by arresting the cells in the G1 phase of the cell cycle, consequently promoting apoptosis and senescence.

3.4 | *DCAF13* deletion suppresses tumor growth *in vivo*

To investigate the role of DCAF13 in breast cancer *in vivo*, we subcutaneously transplanted wild-type or *DCAF13* knockout breast cancer (4T07 and 4T1) cells into both flanks of BALB/c mice. *DCAF13* knockout xenograft-bearing animals exhibited a lower tumor volume and weight compared to the wild-type mice at the end of the experiment (Figure 4A,B). The growth curves provide compelling evidence for stalled tumor cell growth in the *DCAF13* knockout group (Figure 4A,B). Accordingly, data attest that DCAF13 is important for breast cancer development.

In follow-up experiments it was found that levels of DCAF13 and p-histone H3 were significantly reduced in *DCAF13*-deficient tumors (Figure 4C,D), corroborating the link between *DCAF13* deletion and inhibited tumor growth. To elucidate the effect of *DCAF13* deletion on apoptosis *in vivo*, the expression levels of cleaved caspase-3 and the DNA damage marker p-H2AX were examined. Both were highly expressed in *DCAF13*-deficient tumors (Figure 4C,D), which is consistent with the increased p-H2AX associated with *DCAF13* deletion *in vitro* (Figure 2A).

3.5 | Identification of *DCAF13* downstream targets using RNAseq

To understand how *DCAF13* deletion inhibits breast cancer growth, genome-wide RNAseq analysis was performed of wild-type and *DCAF13*-deficient 4T07 cells (Figure 5A). A total of 449 differentially expressed genes were identified in the *DCAF13* knockout group (Figure 5B). Pathway analysis showed that the genes altered by *DCAF13* knockout may play roles in cancer development (Figure 5C). Numerous dysregulated genes that are regulators of cancer cell proliferation and apoptosis were verified by qRT-PCR. For example, *SLC22A18* is an important tumor suppressor gene that encodes an orphan transporter.[20] P53 apoptosis effector related to PMP22 (PERP), a plasma membrane protein, is a transcriptional target of p53 and p63.[21–25] MMP13 is involved in the breakdown of the extracellular matrix.[26]

The expression of *PERP*, *SLC22A18*, *p63*, *ATP13A4*, *MYL9*, *p53*, *CD44*, and *DVL1* in *DCAF13* knockout cells was increased, whereas the expression of *MMP13*, *ELK-1*, *AXIN*, *RASGRP2*, *COL5A3*, and *RASSF4* was decreased (Figures 5D and S2A). Expression of *CK1*, *APC*, *GSK-3β*, and *NOXA* in *DCAF13*-deficient 4T07 cells was unaltered (Figure S2A), while the expression of *PERP*, *SLC22A18*, *p63*, and *p21* was increased in 4T1 *DCAF13* knockout cells (Figure S2A).

Next, we determined whether *DCAF13* deletion induced similar transcriptional dysregulation *in vivo* by qRT-PCR of xenograft biopsies. mRNA levels of *ELK-1* and *MMP13* were decreased, whereas those of *PERP*, *SLC22A18*, and *p63* were increased in 4T07 and 4T1 *DCAF13* knockout xenografts (Figures 5E and S2C). At the protein level, expression of p-H2AX, p-CHK1, GOLPH2, and nucleophosmin was increased in DCAF13 partial knockout cells, whereas the expression of β-catenin and Hp1 was decreased (Figures 5F and S1F).

3.6 | *PERP* is an essential DCAF13 target gene in breast cancer

Both tumor suppressor genes *SLC22A18* and *PERP* are reportedly related to the development of breast cancer.[20,21,27–29] To demonstrate that the observed decrease in *DCAF13* knockout tumor cell proliferation was due to DCAF13-dependent expression of *SLC22A18* or *PERP*, we performed *SLC22A18* and *PERP* knockdown experiments using RNA interference. Both *SLC22A18* and *PERP* mRNA expressions were efficiently suppressed in 4T07 *DCAF13* knockout cells (Figure 6A,B). *SLC22A18* inhibition did not rescue the cell proliferation defect caused by *DCAF13*-deletion (Figure 6C). However, *PERP* inhibition partially rescued the induced *DCAF13*-deficient cell proliferation defects (Figure 6D). To further confirm that *PERP* inhibition could recover the *DCAF13* knockout breast cancer cell proliferation, we established both *PERP*-KO and *DCAF13*-KO breast cancer cells by using CRISPR/Cas9 technology (Figure 6E). The results revealed that *PERP* deletion partially rescued cell proliferation and colony formation in the *DCAF13*-deficient cells (Figure 6F,G).

Through online software analysis (http://ubibrowser.ncpsb.org.cn/ubibrowser/), PERP exhibits multiple ubiquitination sites. We hypothesized that PERP could be recognized and ubiquitinated by $CRL4^{DCAF13}$ E3 ubiquitin ligase. Co-immunoprecipitation showed that DCAF13 directly interacts with PERP (Figure 6H). To identify the interaction domain of DCAF13 with PERP, we used two DCAF13 truncations, in which either the conserved SOF or WD domains of

FIGURE 4 *DCAF13* knockout reduced tumor growth *in vivo*. (A, B) Wild-type and *DCAF13* knockout 4T07 cells (A) and 4T1 cells (B) were injected subcutaneously into both flanks of nude mice (1,000,000 cells per mouse, $N = 6$ per group). The tumor-bearing mice were sacrificed on day 26. Representative photographs of excised tumors are shown in the left panel. The weight of tumors in each group was measured at the end of experiment (middle panel). The tumor volume in each group was measured once every 2 days (right panel). Data are reported as mean ± SE. $^{**}p < 0.01$, $^{***}p < 0.001$ (nonparametric test). (C) Immunohistochemical analysis of DCAF13, p-H2AX, cleaved caspase-3, p-histone H3 in wild-type and *DCAF13* knockout xenografts. (D) The expression levels of the assayed proteins in (C) were analyzed by Western blotting. GAPDH was used as control

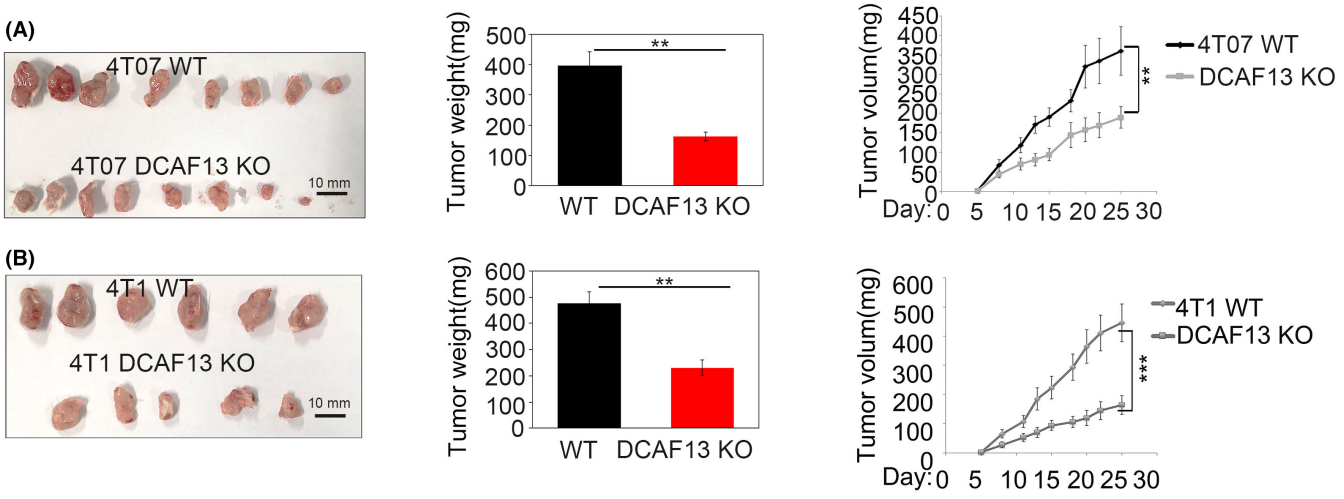

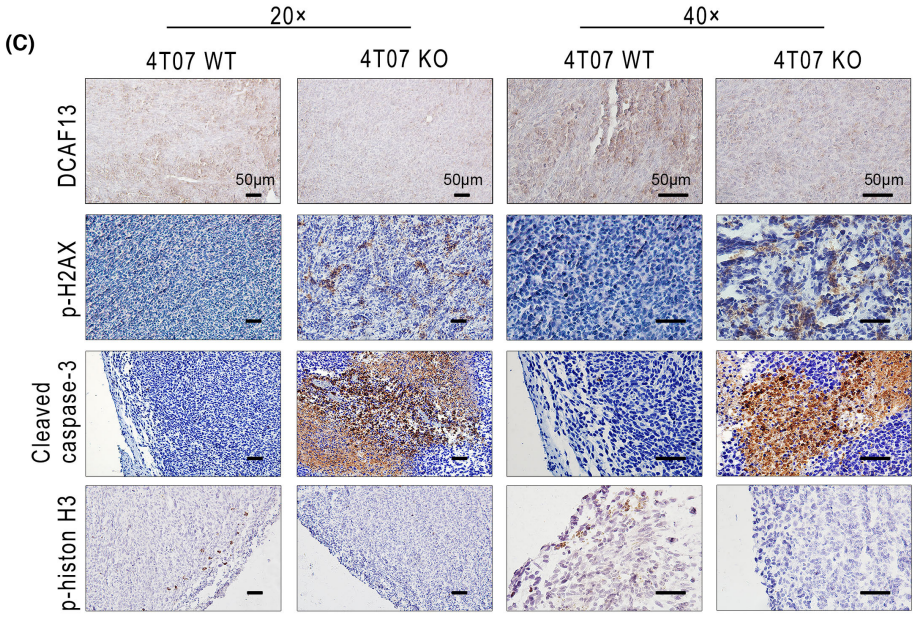

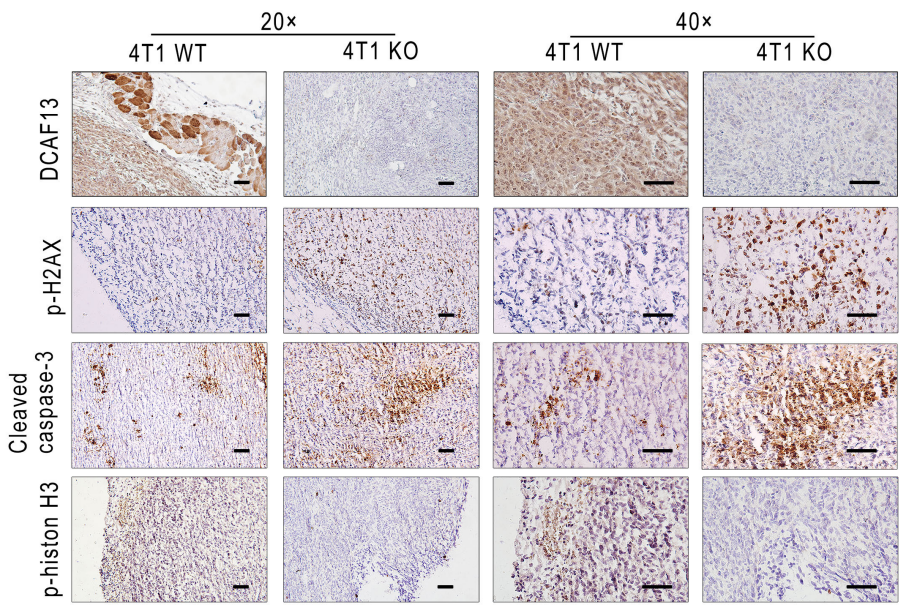

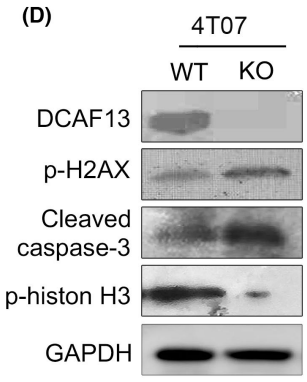

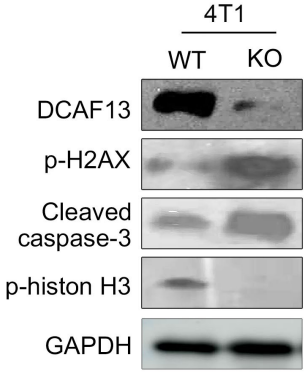

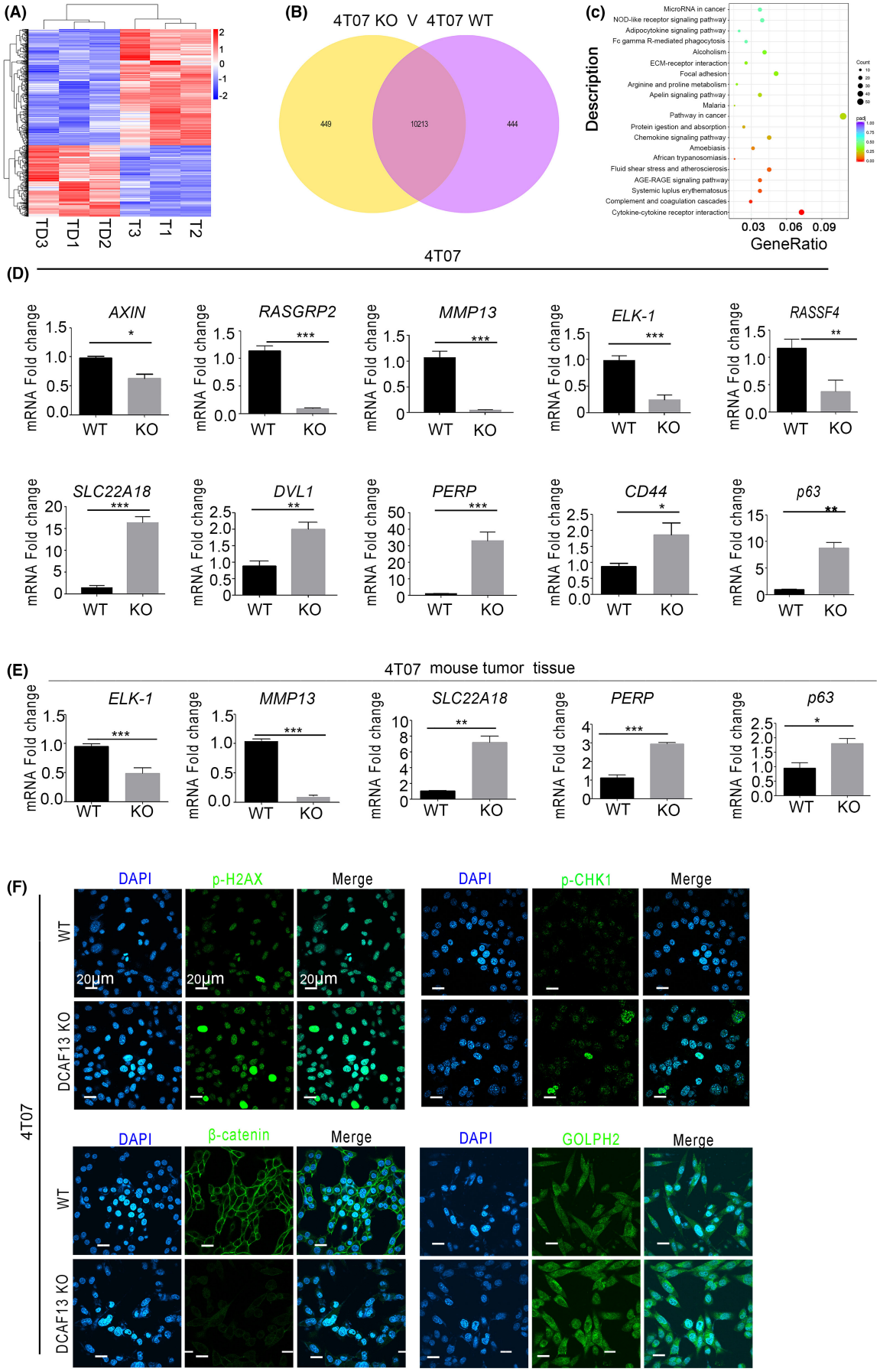

FIGURE 5 Identification of DCAF13 downstream targets by RNAseq. (A) Hierarchical clustering of gene expression profiles from three biologically independent samples based on Pearson correlation coefficient in wild-type and *DCAF13* knockout 4T07 cells. Blue to red signifies weak to strong correlation, respectively. TD1, TD2, and TD3: *DCA13* knockout 4T07 cells; T1, T2, and T3: wild-type 4T07 cells. (B) Gross overview of upregulated genes in wild-type and *DCAF13* knockout 4T07 cells. (C) Differential signaling pathway regulation in *DCAF13* knockout 4T07 cells compared to wild-type cells. (D) RT-PCR analysis of the expression of significantly dysregulated genes in wild-type and *DCAF13* knockout 4T07 cells. Data are presented as mean ± SE ($N = 3$). $^{*}p < 0.05$, $^{**}p < 0.01$, $^{***}p < 0.01$, $^{****}p < 0.001$ (nonparametric test). (E) RT-PCR analysis of the expression of *ELK-1*, *MMP13*, *SLC22A18*, *PERP*, and *p63* in wild-type and *DCAF13* knockout xenografts. (F) Immunofluorescence analysis of p-H2AX, p-CHK1, β-catenin, and GOLPH2 (green) levels in wild-type and DCAF13-deficient 4T07 cells. Cells were counterstained with DAPI (blue)

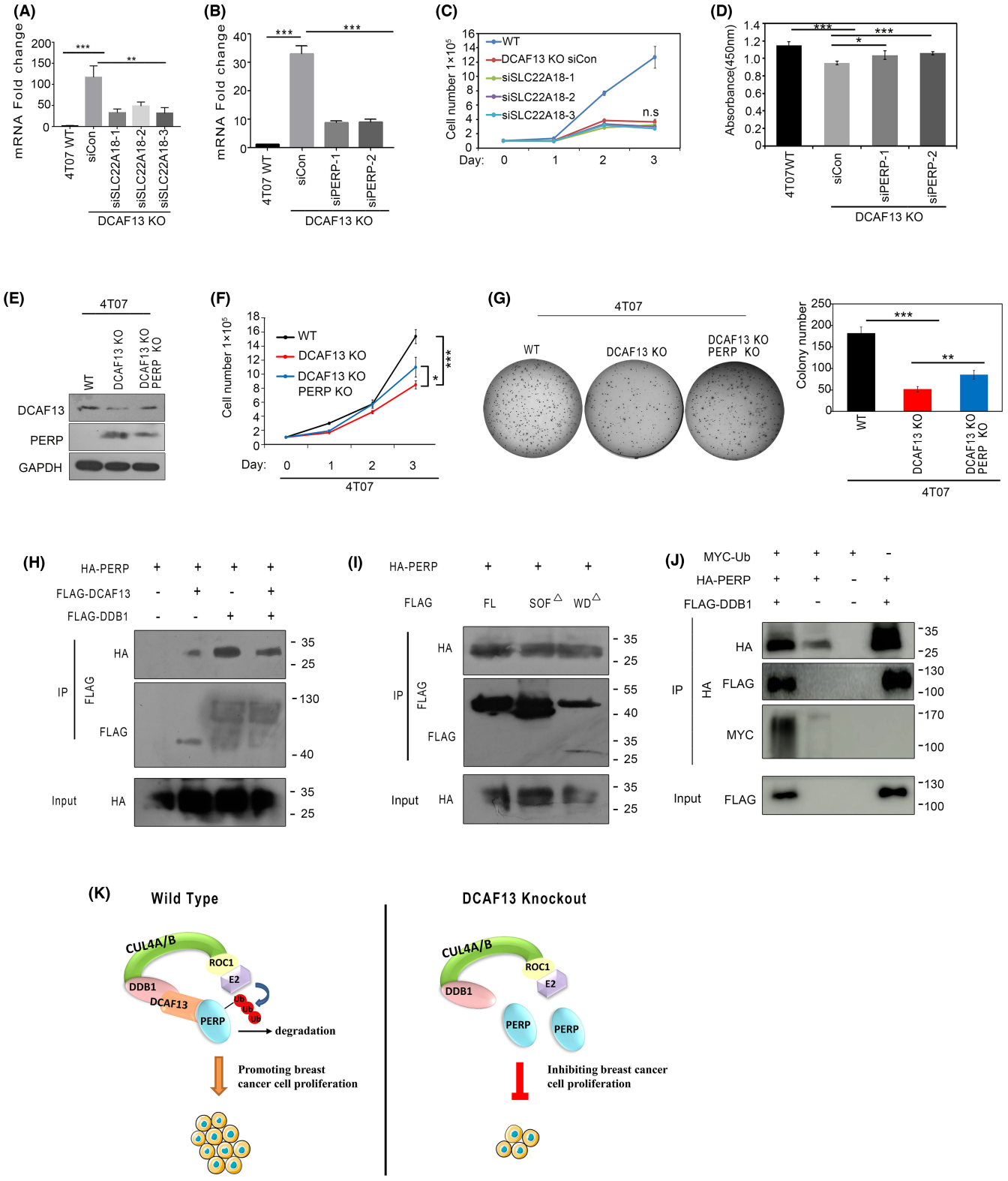

FIGURE 6 PERP is the key target of DCAF13 in breast cancer cell. (A) The mRNA expression level of SLC22A18 in wild-type or *DCAF13* knockout 4T07 cells transfected with control siRNA (siCon) or SLC22A18 siRNAs. $^{**}p < 0.01$, $^{***}p < 0.001$. (B) The mRNA expression level of PERP in 4T07 wild-type cells or *DCAF13* knockout cells transfected with control siRNA (siCon) or PERP siRNAs. $^{***}p < 0.001$. (C) SLC22A18 deletion in *DCAF13* knockout 4T07 cells did not affect cell proliferation. The error bars represent SD ($n = 3$). n.s ($p > 0.05$). Three replicates were included. (D) *PERP* deletion rescues cell proliferation defects in 4T07 DCAF13 KO cells by CCK8 assay. $^{*}p < 0.05$, $^{***}p < 0.001$. (E) Western blotting analysis of the expression of *PERP* in wild-type, *DCAF13* knockout, *DCAF13* knockout and *PERP* knockout 4T07 cells. (F) *PERP* deletion partially rescues the cell growth defects in *DCAF13* knockout 4T07 cells. The error bars represent SD. $^{*}p < 0.05$. $^{***}p < 0.001$. Three replicates were included. (G) *PERP* deletion partially rescues the colony formation defects in DCAF13-deficient cells. Representative images from the colony formation assay (left panel) and the colony number analysis (right panel) were shown. All experiments were performed in triplicate. $^{**}p < 0.01$, $^{***}p < 0.001$ (H) Co-immunoprecipitation result showing PERP interacts with DCAF13 and DDB1. 293T cells transfected with plasmids encoding the indicated proteins were lysed and subjected to IP with anti-Flag beads. Input lysates was immunoblotted with antibodies against HA. (I) 293T cells transiently transfected with plasmids encoding the full-length Flag-DCAF13 or the DCAF13 two truncations (Flag-DCAF13 SOF$^{\triangle}$ and Flag-DCAF13 WD$^{\triangle}$) together with HA-PERP. Protein extracts were immunoprecipitated using anti-Flag beads. (J) Co-immunoprecipitation experiments showing *PERP* polyubiquitination. (K) A working model explaining how DCAF13 promotes breast cancer cell proliferation. In wild-type breast cancer cell, PERP, a tumor suppressor protein, is polyubiquitinated by CRL4DCAF13 and destabilized. This promotes the proliferation of breast cancer cell. When DCAF13 was knocked out, PERP could not be polyubiquitinated and became stabilized, resulting in the inhibition of breast cancer cell proliferation

DCAF13 were deleted and found that both the DCAF13 SOF$^{\triangle}$ and WD$^{\triangle}$ truncations interacted with PERP, suggesting that these two domains are not involved in the interaction (Figure 6I). Given that DCAF13 functions as a substrate receptor protein for CRL4 E3 ubiquitin ligase complex, we further explored whether PERP acts as a substrate for CRL4 E3 ubiquitin ligase. We then examined the association between PERP and DDB1, the linker protein of CRL4 E3 ligase. PERP interacted with DDB1, suggesting that PERP could form complexes with CRL4^{DCAF13} E3 ligase (Figure 6H). Moreover, overexpression of *DDB1* significantly increased the polyubiquitination of PERP (Figure 6J), suggesting that CRL4^{DCAF13} E3 ligase targets PERP for ubiquitination and proteasomal degradation.

4 | DISCUSSION

Several studies support the possibility of *DCAF13* being an oncogene.[14,16–18] *DCAF13* has been reported to be overexpressed in hepatocellular carcinoma, and its overexpression is significantly associated with poor survival in patients with hepatocellular carcinoma.[16] *DCAF13* was also significantly upregulated in human lung adenocarcinomas, and knockdown of *DCAF13* inhibited human lung adenocarcinoma cell migration.[17] Through DCAF13, CRL4 E3 ligase specifically recognizes the tumor suppressor PTEN for degradation.[13,14] Consistent with these reports, our present work illustrates that *DCAF13* is a potential oncogene in breast cancer. We found that *DCAF13* was significantly upregulated in breast cancer tissues. *DCAF13* deletion resulted in defects in cell proliferation, colony formation, and migration, induced cell cycle arrest at G1/S phase, and increased cell apoptosis. A recent study by Liu demonstrates that DCAF13 promotes triple-negative breast cancer metastasis.[18] Consistent with Liu's study, we found that a high expression of *DCAF13* in breast cancer tissues was closely correlated with overall survival. In addition, our study not only revealed that *DCAF13* promotes breast cancer metastasis, but also contributes to cell proliferation, apoptosis, and senescence. Importantly, we elucidate a new molecular mechanism by which CRL4^{DCAF13} E3 ligase targets polyubiquitination and degradation of PERP.

P53 apoptosis effector related to PMP22 was identified as the transcriptional downstream protein of p63.[29,30] It acts as a tumor suppressor protein downregulated in several human cancers.[31] In recent years, many studies have confirmed a link between low PERP protein levels and the development of various cancers, including breast cancer, squamous cell carcinoma, and papillary thyroid cancer.[21–25] PERP has multifaceted role in cancer, involving apoptosis, cell–cell adhesion, epithelial–mesenchymal transition, and Ca^{2+} signaling.[21,29,32] We found that PERP expression was increased in *DCAF13*-deficient breast cancer cells and *PERP* inhibition partially rescued the proliferation of *DCAF13*-deficient breast cancer cells, supporting that DCAF13 promotes breast cancer cell proliferation by inhibiting *PERP* expression. Co-immunoprecipitation showed DCAF13 interacts with PERP, and overexpression of DDB1 enhances the polyubiquitination of PERP, indicating that CRL4^{DCAF13} E3 ligases targets PERP for ubiquitination. However, CRL4^{DCAF13}-mediated PERP degradation needs examination. Human DCAF13s are nucleolar proteins. PERP is enriched in the plasma membrane and contributes to cell–cell contacts. Thus, it is necessary for DCAF13 translocation from nucleus to the cytoplasm. The mechanism that PERP regulates breast cancer cell proliferation needs to be further investigated. Taken together, DCAF13 promotes the breast cancer cell proliferation partially by inhibiting the activity of PERP. DCAF13 should be considered for the development of novel drugs targeting breast cancer.

RNAseq analysis of the *DCAF13*-deficiency-related transcriptome indicated that DCAF13 activated multiple signaling pathways, including the Wnt/β-catenin pathway and PI3K-AKT pathways. The Wnt/β-catenin pathway has been reported to play an important role in cancer progression.[33,34] Thus, *DCAF13* knockout may exert a suppressive effect on cellular behaviors by inactivating the Wnt/β-catenin pathway. In addition, Zhang et al. demonstrated that CRL4^{DCAF13} E3 ubiquitin ligase targets the polyubiquitination and degradation of PTEN,[13] an inhibitor of PI3K-AKT signaling pathway, thereby maintaining the activity of AKT activity and promoting oocytes meiotic maturation, implying that *DCAF13* deletion leads to the inactivation of AKT activity.

In summary, our study not only revealed critical roles of DCAF13 in the growth and metastasis of breast cancer but also highlighted the mechanism where $CRL4^{DCAF13}$ E3 ligase mediates PERP degradation and promotes breast cancer cell proliferation, as illustrated in Figure 6K. This study indicated that DCAF13 could be a potential target for breast cancer diagnosis and treatment. It may be expedient to silence the expression of *DCAF13* for the purpose of treating breast cancer. In the field of cancer therapy, small interfering RNA (siRNA) intervention is considered as a powerful tool for gene silencing (knockdown), enabling the suppression of oncogenic factors in cancer.[35] Our findings provide evidence for future breast cancer therapy by inhibiting *DCAF13* with siRNAs. Although siRNA intervention has been applied to the treatment of breast cancer,[36] siRNA-based therapies have not yet reached the clinic, but with further development of multiple targets, sophisticated delivery systems, and combination treatments, hopefully a breakthrough can be achieved.

ACKNOWLEDGEMENTS

This work was supported by the National Natural Science Foundation of China (31871402, 31701260), the Natural Science Foundation of Zhejiang Province (LY21H160047, LY17H160060, LGD21H160003, LZ20H16004), the Jiaxing Science and Technology Bureau project (2020AD10018, 2020AD30073, 00320117AL), the Jiaxing Key Laboratory for Photonanomedicine and Experimental Therapeutics (12.2019), the Zhejiang Provincial Foreign Expert Grant (12.2018), the Dutch Cancer Foundation (KWF, 10666), the Jiaxing University Scientific Research Start-up project (CD70519018), the National College Student Innovation and Entrepreneurship Training Program (202010354043, 202010354042, 2020R417015, 202110354015, 2021R417023, 2021R417028, 202113291002, 202113291003), the Jiaxing talent pioneer innovation team, and the key Laboratory of Medical Electronics and Digital Health of Zhejiang Province.

DISCLOSURE

The authors declare no potential conflicts of interest.

ORCID

Xiao-Min Wang https://orcid.org/0000-0001-7128-8097
Shu-Qun Cheng https://orcid.org/0000-0001-6760-7470

REFERENCES

1. Akram M, Iqbal M, Daniyal M, et al. Awareness and current knowledge of breast cancer. *Biol Res*. 2017;50:33. doi:10.1186/s40659-017-0140-9
2. Sung H, Ferlay J, Siegel RL, et al. Global cancer statistics 2020: GLOBOCAN estimates of incidence and mortality worldwide for 36 cancers in 185 countries. *CA Cancer J Clin*. 2021;71:209-249. doi:10.3322/caac.21660
3. Gooding AJ, Parker KA, Valadkhan S, et al. The lncRNA BORG: a novel inducer of TNBC metastasis, chemoresistance, and disease recurrence. *J Cancer Metastasis Treat*. 2019;5:41. doi:10.20517/2394-4722.2019.11
4. Tu Y, Chen C, Pan J, et al. The ubiquitin proteasome pathway (UPP) in the regulation of cell cycle control and DNA damage repair and its implication in tumorigenesis. *Int J Clin Exp Pathol*. 2012;5:726-738.
5. Cheng J, Guo J, North BJ, et al. The emerging role for Cullin 4 family of E3 ligases in tumorigenesis. *Biochim Biophys Acta Rev Cancer*. 2019;1871:138-159. doi:10.1016/j.bbcan.2018.11.007
6. Zimmerman ES, Schulman BA, Zheng N. Structural assembly of cullin-RING ubiquitin ligase complexes. *Curr Opin Struct Biol*. 2010;20:714-721. doi:10.1016/j.sbi.2010.08.010
7. Chen Z, Sui J, Zhang F, Zhang C. Cullin family proteins and tumorigenesis: genetic association and molecular mechanisms. *J Cancer*. 2015;6:233-242. doi:10.7150/jca.11076
8. Ni W, Zhang Y, Zhan Z, et al. A novel lncRNA uc.134 represses hepatocellular carcinoma progression by inhibiting CUL4A-mediated ubiquitination of LATS1. *J Hematol Oncol*. 2017;10:91. doi:10.1186/s13045-017-0449-4
9. Benamar M, Guessous F, Du K, et al. Inactivation of the CRL4-CDT2-SET8/p21 ubiquitylation and degradation axis underlies the therapeutic efficacy of pevonedistat in melanoma. *EBioMedicine*. 2016;10:85-100. doi:10.1016/j.ebiom.2016.06.023
10. Higa LA, Wu M, Ye T, et al. CUL4-DDB1 ubiquitin ligase interacts with multiple WD40-repeat proteins and regulates histone methylation. *Nat Cell Biol*. 2006;8:1277-1283. doi:10.1038/ncb1490
11. Ren W, Shen S, Sun Z, et al. Jak-STAT3 pathway triggers DICER1 for proteasomal degradation by ubiquitin ligase complex of CUL4A(DCAF1) to promote colon cancer development. *Cancer Lett*. 2016;375:209-220. doi:10.1016/j.canlet.2016.02.055
12. Huang J, Chen J. VprBP targets merlin to the Roc1-Cul4A-DDB1 E3 ligase complex for degradation. *Oncogene*. 2008;27:4056-4064. doi:10.1038/onc.2008.44
13. Zhang J, Zhang YL, Zhao LW, et al. Mammalian nucleolar protein DCAF13 is essential for ovarian follicle maintenance and oocyte growth by mediating rRNA processing. *Cell Death Differ*. 2019;26:1251-1266. doi:10.1038/s41418-018-0203-7
14. Chen Z, Zhang W, Jiang K, et al. MicroRNA-300 regulates the ubiquitination of PTEN through the CRL4B(DCAF13) E3 ligase in osteosarcoma cells. *Mol Ther Nucleic Acids*. 2018;10:254-268. doi:10.1016/j.omtn.2017.12.010
15. Zhang J, Zhang YL, Zhao LW, et al. The CRL4-DCAF13 ubiquitin E3 ligase supports oocyte meiotic resumption by targeting PTEN degradation. *Cell Mol Life Sci*. 2020;77:2181-2197. doi:10.1007/s00018-019-03280-5
16. Cao J, Hou P, Chen J, et al. The overexpression and prognostic role of DCAF13 in hepatocellular carcinoma. *Tumour Biol*. 2017;39:1010428317705753. doi:10.1177/1010428317705753
17. Yan H, Bi L, Wang Y, et al. Integrative analysis of multi-omics data reveals distinct impacts of DDB1-CUL4 associated factors in human lung adenocarcinomas. *Sci Rep*. 2017;7:333. doi:10.1038/s41598-017-00512-1
18. Liu J, Li H, Mao A, et al. DCAF13 promotes triple-negative breast cancer metastasis by mediating DTX3 mRNA degradation. *Cell Cycle*. 2020;19:3622-3631. doi:10.1080/15384101.2020.1859196
19. Pan WW, Zhou JJ, Yu C, et al. Ubiquitin E3 ligase CRL4(CDT2/DCAF2) as a potential chemotherapeutic target for ovarian surface epithelial cancer. *J Biol Chem*. 2013;288:29680-29691. doi:10.1074/jbc.M113.495069
20. Ito S, Fujino Y, Ogata S, et al. Involvement of an orphan transporter, SLC22A18, in cell growth and drug resistance of human breast cancer MCF7 cells. *J Pharm Sci*. 2018;107:3163-3170. doi:10.1016/j.xphs.2018.08.011
21. Khan IA, Yoo BH, Masson O, et al. ErbB2-dependent downregulation of a pro-apoptotic protein perp is required for oncogenic transformation of breast epithelial cells. *Oncogene*. 2016;35:5759-5769. doi:10.1038/onc.2016.109
22. Kong CS, Cao H, Kwok S, et al. Loss of the p53/p63 target PERP is an early event in oral carcinogenesis and correlates with higher rate of local relapse. *Oral Surg Oral Med Oral Pathol Oral Radiol*. 2013;115:95-103. doi:10.1016/j.oooo.2012.10.017

23. Zhai T, Muhanhali D, Jia X, et al. Identification of gene co-expression modules and hub genes associated with lymph node metastasis of papillary thyroid cancer. *Endocrine*. 2019;66:573-584. doi:10.1007/s12020-019-02021-9
24. Paraoan L, Gray D, Hiscott P, et al. Expression of p53-induced apoptosis effector PERP in primary uveal melanomas: downregulation is associated with aggressive type. *Exp Eye Res*. 2006;83:911-919. doi:10.1016/j.exer.2006.04.016
25. Dusek RL, Bascom JL, Vogel H, et al. Deficiency of the p53/p63 target perp alters mammary gland homeostasis and promotes cancer. *Breast Cancer Res*. 2012;14:R65. doi:10.1186/bcr3171
26. Pittayapruek P, Meephansan J, Prapapan O, et al. Role of matrix metalloproteinases in photoaging and photocarcinogenesis. *Int J Mol Sci*. 2016;17:868. doi:10.3390/ijms17060868
27. He H, Xu C, Zhao Z, et al. Low expression of SLC22A18 predicts poor survival outcome in patients with breast cancer after surgery. *Cancer Epidemiol*. 2011;35:279-285. doi:10.1016/j.canep.2010.09.006
28. Gallagher E, Mc Goldrick A, Chung WY, et al. Gain of imprinting of SLC22A18 sense and antisense transcripts in human breast cancer. *Genomics*. 2006;88:12-17. doi:10.1016/j.ygeno.2006.02.004
29. Roberts O, Paraoan L. PERP-ing into diverse mechanisms of cancer pathogenesis: regulation and role of the p53/p63 effector PERP. *Biochim Biophys Acta Rev Cancer*. 2020;1874:188393. doi:10.1016/j.bbcan.2020.188393
30. Awais R, Spiller DG, White MR, et al. p63 is required beside p53 for PERP-mediated apoptosis in uveal melanoma. *Br J Cancer*. 2016;115:983-992. doi:10.1038/bjc.2016.269
31. Hildebrandt T, Preiherr J, Tarbé N, et al. Identification of THW, a putative new tumor suppressor gene. *Anticancer Res*. 2000;20:2801-2809.
32. McDonnell SJ, Spiller DG, White MRH, et al. ER stress-linked autophagy stabilizes apoptosis effector PERP and triggers its co-localization with SERCA2b at ER-plasma membrane junctions. *Cell Death Discov*. 2019;5:132. doi:10.1038/s41420-019-0212-4
33. Krishnamurthy N, Kurzrock R. Targeting the Wnt/beta-catenin pathway in cancer: update on effectors and inhibitors. *Cancer Treat Rev*. 2018;62:50-60. doi:10.1016/j.ctrv.2017.11.002
34. Bugter JM, Fenderico N, Maurice MM. Mutations and mechanisms of WNT pathway tumour suppressors in cancer. *Nat Rev Cancer*. 2021;21:5-21. doi:10.1038/s41568-020-00307-z
35. Ashrafizadeh M, Hushmandi K, Rahmani Moghadam E, et al. Progress in delivery of siRNA-based therapeutics employing nanovehicles for treatment of prostate cancer. *Bioengineering (Basel)*. 2020;7:91. doi:10.3390/bioengineering7030091
36. Yang C, Cheng X, Shen P. Silencing of BCSG1 with specific siRNA via nanocarriers for breast cancer treatment. *Bull Cancer*. 2021;108:323-332. doi:10.1016/j.bulcan.2020.10.022

SUPPORTING INFORMATION

Additional supporting information may be found in the online version of the article at the publisher's website.

How to cite this article: Shan B-Q, Wang X-M, Zheng L, et al. DCAF13 promotes breast cancer cell proliferation by ubiquitin inhibiting *PERP* expression. *Cancer Sci*. 2022;113:1587–1600. doi:10.1111/cas.15300